Jurnal Pendidikan dan Ilmu Fisika (JPIF)
Fakultas Pendidikan Islam dan Keguruan
Universitas Garut
p-ISSN: 2798-9488 e-ISSN: 2798-334X

Python-Based Image Segmentation for Corona Plasma Ozone Microbubbles Diameter Analysis

Anggyta Fitryan[1*], Ahmad Faruq Abdurrahman[2], Junaidi[3], Sri Wahyu Suciati[4]

[1,2,3,4]Program Studi Fisika, Fakultas Matematika dan Ilmu Pengetahuan Alam
Universitas Lampung, Indonesia
Jl. Prof. Dr. Sumantri Brojonegoro No.1, Bandar Lampung

[1]*e-mail: fr.agyta21@gmail.com

DOI:
https://doi.org/10.52434/jpif.v6i1.44008

Accepted: June 18, 2026, Approved: June 20, 2026, Published: June 22, 2026

ABSTRACT

Accurate measurement of microbubble size is an essential step in evaluating the performance of corona-discharge-based ozone systems because bubble diameter distribution strongly influences interfacial area and mass transfer efficiency. This study aimed to develop a Python-based application for automatic microbubble diameter analysis using digital image segmentation. The program was developed by integrating OpenCV, NumPy, Pillow, Tkinter, and Matplotlib to support image loading, region-of-interest selection, preprocessing, thresholding, contour detection, visualization, and bubble diameter calculation. Size calibration was performed using a field-of-view approach based on camera sensor parameters and lens magnification to determine the pixel-to-micrometer conversion factor. Bubble diameter was calculated using the equivalent circular diameter derived from the segmented contour area. The developed application successfully distinguished bubble populations generated by two ozone diffusers, producing average diameters of 4.09 μm for the C-50 diffuser and 3.37 μm for the C-80 diffuser. These results demonstrate that the program can automatically detect microbubbles and provide systematic size distribution for laboratory-scale image analysis. The proposed application offers a practical, transparent, and open-source solution for rapid microbubble diameter measurement and has potential for broader application in gas–liquid bubble image analysis.

Keywords: Diameter analysis, Image segmentation, Microbubble, OpenCV, Python

Segmentasi Citra Berbasis Python untuk Analisis Diameter Gelembung Mikro Ozon Plasma Korona

ABSTRAK

Pengukuran microbubble secara akurat merupakan tahap penting dalam mengevaluasi kinerja sistem ozon berbasis corona discharge karena distribusi diameter gelembung sangat memengaruhi luas permukaan kontak dan efisiensi transfer massa. Penelitian ini bertujuan mengembangkan aplikasi berbasis Python untuk menganalisis diameter microbubble secara otomatis menggunakan metode segmentasi citra digital. Program dikembangkan dengan mengintegrasikan pustaka OpenCV, NumPy, Pillow, Tkinter, dan Matplotlib untuk mendukung proses pemuatan citra, pemilihan region of interest (ROI), prapemrosesan, thresholding, deteksi *kontur, visualisasi hasil, dan perhitungan diameter gelembung. Kalibrasi ukuran dilakukan menggunakan pendekatan field of view berdasarkan parameter sensor kamera dan perbesaran lensa untuk menentukan faktor konversi piksel ke mikrometer. Diameter gelembung dihitung menggunakan metode diameter ekuivalen lingkaran berdasarkan luas kontur hasil segmentasi. Aplikasi yang dikembangkan berhasil membedakan populasi gelembung yang dihasilkan oleh dua jenis diffuser ozon, dengan diameter rata-rata sebesar 4,09 µm pada diffuser C-50 dan 3,37 µm pada diffuser C-80. Hasil tersebut menunjukkan bahwa program mampu mendeteksi microbubble secara otomatis serta menyajikan distribusi ukuran secara sistematis untuk analisis citra skala laboratorium. Aplikasi yang dikembangkan menawarkan solusi yang praktis, transparan, dan berbasis open-source untuk pengukuran diameter microbubble secara cepat serta berpotensi diterapkan pada analisis citra gelembung dalam berbagai sistem gas-cair.*

***Kata kunci**: Analisis diameter, Gelembung mikro, OpenCV, Python, Segmentasi citra*

INTRODUCTION

Image segmentation is a core operation in image processing and computer vision because it divides an image into meaningful, non-overlapping regions that can be used for subsequent object-level analysis (Cheng et al., 2023). Classic segmentation strategies still remain important in practical measurement systems, especially when the target object has a relatively simple foreground–background structure and the user needs interpretable processing steps rather than a black-box prediction (Cheng et al., 2023; Jardim et al., 2023).

Thresholding is particularly attractive for scientific imaging because it is computationally light, easy to reproduce, and effective when the contrast between object and background can be controlled during acquisition (Jardim et al., 2023). For bubble imagery, however, segmentation becomes difficult when lighting varies, object edges are weak, or multiple bubbles overlap inside a single frame. Studies on bubbly flow have shown that conventional pipelines frequently require manual trial-and-error in threshold selection, which increases operator dependence and reduces reproducibility across datasets and optical conditions (Chen et al., 2022; Kim & Park, 2021). At the same time, optical visualization remains one of the most useful non-intrusive approaches for extracting bubble shape and size information in multiphase-flow experiments (Kim & Park, 2021; Lewandowski et al., 2018). The computational problem is therefore not only to detect bubbles, but also to transform segmented regions into reliable geometric descriptors such as equivalent diameter, contour area, and distribution statistics (Lewandowski et al., 2018).

Recent open-source measurement platforms implemented in Python demonstrate that transparent software design, direct user control, and modular numerical libraries are well suited to laboratory-scale image analysis workflows. Python-based tools commonly combine OpenCV for preprocessing and contour extraction, NumPy for array operations, and graphical interfaces that let users adjust calibration and select the region of interest without leaving the same workflow (Filho et al., 2022; Harikrishna et al., 2025). In addition, automated image-based diameter measurement has been validated in other domains, showing that segmentation quality strongly determines the reliability of downstream size estimation (Hotaling et al., 2015; Lewandowski et al., 2018).

The performance of ozone microbubble systems is strongly influenced by bubble characteristics, particularly bubble diameter. Bubble size determines the gas-liquid interfacial area, bubble residence time, and ozone mass transfer efficiency, thereby directly affecting oxidation and disinfection performance. Previous studies have demonstrated that ozone microbubbles provide higher volumetric mass transfer coefficients (kLa) and better ozone utilization efficiency than conventional bubbles. However, most existing studies focus primarily on evaluating ozonation performance, while automated image-based characterization of microbubble diameter remains limited. Therefore, the development of a Python-based image segmentation method is important to enable rapid, objective, and consistent measurement of microbubble diameter for evaluating the performance of corona plasma ozone microbubble generators (John et al., 2022; Xiong et al., 2019).

Although many image segmentation methods have been developed for bubble analysis, most previous studies emphasize segmentation algorithms or deep-learning approaches rather than providing a lightweight, open-source application that integrates calibration, ROI selection, diameter computation, visualization, and data export in a single workflow. Therefore, this study develops a Python-based application specifically designed for laboratory-scale ozone microbubble diameter analysis.

Based on this research gap, this study focuses on the development of a Python-based application for automatic microbubble diameter analysis from digital images. The objective of this study is to describe the application architecture, segmentation workflow, calibration procedure, and measurement outputs for laboratory-scale corona-discharge ozone microbubble experiments.

METHOD

The input images were captured using an handphone (Phone 11) combined with a 40 mm macro lens with 12.5x magnification. The captured frames contained ozone microbubbles produced by two diffusers, namely C-50 and C-80, and were processed individually through the Python application.

The minimum measurable bubble size is fundamentally constrained by the optical resolution of the imaging system. According to the (Rayleigh, 1879) criterion, diffraction limits the ability of an optical system to distinguish closely spaced objects. In conventional optical microscopy, this diffraction limit is typically on the order of hundreds of nanometers and is governed by the point spread function of the imaging system. In practice, the effective resolution is further influenced by image contrast, optical aberrations, and signal-to-noise ratio. Consequently, bubbles approaching the optical resolution limit may appear blurred or merged, reducing segmentation accuracy and affecting diameter estimation (Huang et al., 2009; Stelzer, 1998).

In this study, Tkinter was used to build the graphical user interface, PIL to display images, OpenCV to preprocess and segment images, NumPy and math for numerical computation, Matplotlib to plot diameter distributions, and csv plus datetime modules for structured data export.

The interface was arranged into three functional zones: a left panel for controls and calibration inputs, a central panel for the original image and the segmentation result, and a right panel for tabulated bubble measurements and histogram visualization.

First, the image was loaded and optionally cropped into a region of interest so that the measurement focused only on the bubble field. Second, the selected image was converted into a form suitable for binary segmentation. Third, thresholding and contour detection were applied to isolate candidate bubbles. Finally, each contour area was converted into an equivalent circular diameter. The main processing stages implemented in the program can be seen in Table 1.

Table 1. The main processing stages

Stage	Function in the program
Image input and ROI	Loads the image and limits the analysis area to the relevant bubble field
Preprocessing (CLAHE + Gaussian)	Enhances local contrast and reduces image noise before segmentation
Adaptive Gaussian thresholding	Segments bubble regions using adapive local thresholding under non-uniform ilumination
Contour extraction	Detects each segmented object and computes contour area
Morphological opening	Removes isolated noise and refines binary objects before contour detection
Contour extraction	Detech each segmented bubble and computes its contour area
Calibration	Converts pixel dimensions into micrometers using field-of-view scaling
Equivalent diameter calculation	Computes the area-equivalent bubble diameter from the contour area
Output and visualization	Displays segmented results, tables, histograms, and exportable records

The calibration procedure was based on the field-of-view relation used in the code. The field of view (FOV) in millimeters is given by Equation (1).

$$FOV = Sensor\ Width\ /\ Magnification \qquad ...(1)$$

After the FOV is known, the pixel-to-micrometer ratio is computed from the image width, as shown in Equation (2).

$$Pixel\ Scale\ (\mu m/pixel) = (FOV \times 100)\ /\ Image\ Width \qquad ...(2)$$

For each segmented contour, the program calculates the area-equivalent diameter by assuming a circle with the same projected area, as shown in Equation (3). This representation is widely used in image-based diameter estimation because it yields a simple and comparable scalar size metric for irregular projections (Lewandowski et al., 2018).

$$d = 2 \times \sqrt{\frac{A}{\pi}} \qquad ...(3)$$

RESULT AND DISCUSSION

The developed application produced an operational workflow for laboratory image analysis rather than a single-use script. The user can load images, inspect the original frame, run segmentation, review contour-based detections, and read the corresponding diameter statistics from the same interface. The results of the analysis of ozone microbubble size are shown in the Figure 1 and Figure 2.

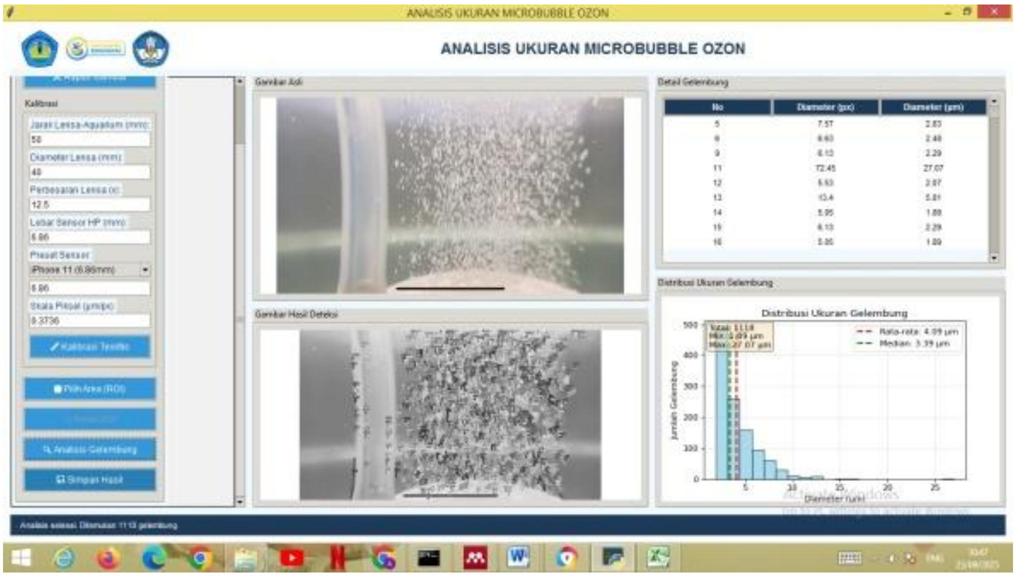

ANALISIS UKURAN MICROBUBBLE OZON

Kalibrasi

Jarak Lensa-Aquarium (mm): 50
Diameter Lensa (mm): 40
Perbesaran Lensa (x): 12.5
Lebar Sensor HP (mm): 6.86
Preset Sensor: iPhone 11 (6.86mm)
6.86
Skala Piksel (µm/px): 0.3736

Detail Gelembung

No	Diameter (px)	Diameter (µm)
5	7.57	2.83
8	6.63	2.48
9	6.13	2.29
11	72.45	27.07
12	5.53	2.07
13	13.4	5.01
14	5.05	1.89
15	6.13	2.29
16	5.05	1.89

Analisis selesai. Ditemukan 1118 gelembung.

Figure 1. Analysis of C-50 difusser

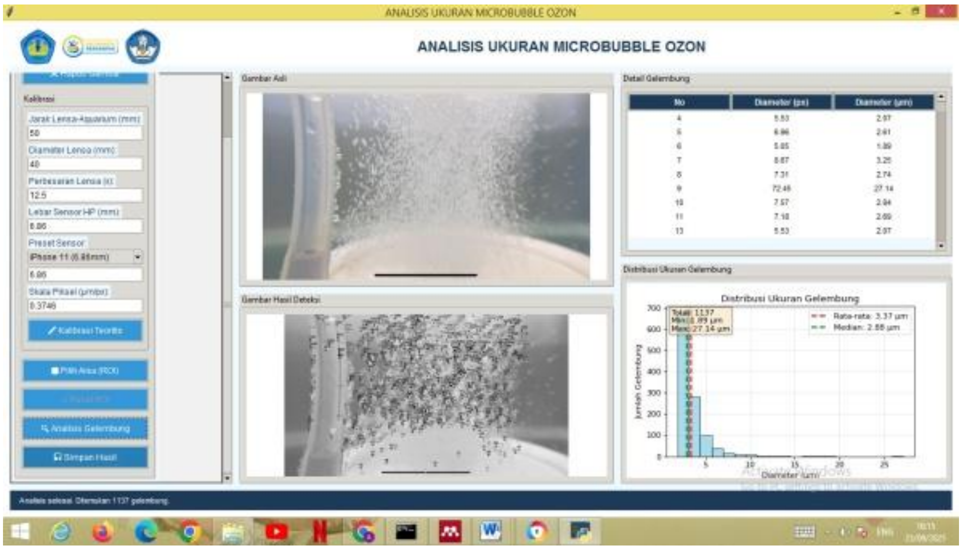

ANALISIS UKURAN MICROBUBBLE OZON

Kalibrasi

Jarak Lensa-Aquarium (mm): 50
Diameter Lensa (mm): 40
Perbesaran Lensa (x): 12.5
Lebar Sensor HP (mm): 6.86
Preset Sensor: iPhone 11 (6.86mm)
6.86
Skala Piksel (µm/px): 0.3746

Detail Gelembung

No	Diameter (px)	Diameter (µm)
4	5.53	2.07
5	6.96	2.61
6	5.05	1.89
7	8.67	3.25
8	7.31	2.74
9	72.45	27.14
10	7.57	2.84
11	7.18	2.69
13	5.53	2.07

Analisis selesai. Ditemukan 1137 gelembung.

Figure 2. Analysis of C-80 difusser

The main measurement results for microbubbles from the program, as shown in Figure 1 and Figure 2, are presented in Table 2**.**

Table 2. The main measurement output

Sample	Mean diameter (µm)	Interpretation
C-50 diffuser	4.09	Produced larger average bubbles in the analyzed image set.
C-80 diffuser	3.37	Produced smaller and more desirable microbubble diameters.

The measured values indicate that program was sensitive enough to differentiate the two diffuser conditions, indicating that the proposed image segmentation method can reliably detect differences in microbubble diameter distributions resulting from variations in diffuser configuration. Such observations are important because bubble size strongly influences gas–liquid mass transfer, reactive species generation, and the overall performance of plasma microbubble systems (Hong et al., 2021; John et al., 2022). In the context of the present image dataset, the C-80 diffuser yielded a smaller mean diameter than the C-50 diffuser, which is consistent with the expectation that the program can resolve relative differences between bubble populations.

Another important outcome is the visual feedback provided by the segmented result, the labeled detections, and the histogram. These outputs help the user inspect whether the measured objects correspond to actual bubbles, which is essential because segmentation errors propagate directly into size statistics (Hotaling et al., 2015).

The code nevertheless has identifiable limitations. Overlapping bubbles can merge into a single contour, out-of-focus objects can distort threshold boundaries, and fast-moving bubbles may appear non-circular in a single captured frame. Similar issues have also been emphasized in recent bubble-segmentation studies, where clustered objects, unstable illumination, and irregular shapes remain major challenges. For this reason, the present program should be interpreted as a robust classical segmentation workflow for controlled images, not as a universal detector for all bubbly-flow scenes. If the dataset becomes denser, noisier, or more heterogeneous, methods such as adaptive watershed separation or deep instance segmentation may become more appropriate (Chen et al., 2022; Kim & Park, 2021).

Even so, the present program offers a strong practical contribution for student-scale and laboratory-scale research because it is transparent, low-cost, and based on open-source components. The combination of GUI-based interaction, explicit calibration, and automatic equivalent-diameter computation makes the system suitable for reproducible microbubble analysis without specialized commercial software.

CONCLUSION

This study developed a Python-based application for automated microbubble diameter measurement using digital image segmentation. The program integrates image loading, region-of-interest selection, preprocessing, threshold-based segmentation, contour extraction, calibration, equivalent diameter calculation, and data visualization within a single workflow. The use of area-equivalent diameter provides a reproducible quantitative metric for bubble size estimation from segmented images.

The application successfully analyzed images obtained from two diffuser conditions (C-50 and C-80) and produced consistent diameter distributions that were sufficiently different to distinguish the two diffuser characteristics. These results demonstrate that the developed workflow can support objective and repeatable laboratory-scale microbubble characterization while reducing the subjectivity associated with manual measurements.

The present implementation is intended for images acquired under controlled illumination and imaging conditions, where threshold-based segmentation provides reliable bubble detection. Future work should focus on improving robustness for images with non-uniform illumination, overlapping bubbles, and varying image quality by incorporating adaptive thresholding or machine learning-based segmentation methods. In addition, validation against independent measurement techniques would further strengthen the accuracy and applicability of the proposed program.

REFERENCES

Chen, B., Ekwonu, M. C., & Zhang, S. (2022). Deep learning-assisted segmentation of bubble image shadowgraph. *Journal of Visualization*, *25*(6), 1125–1136. https://doi.org/10.1007/s12650-022-00849-4

Cheng, J., Li, H., Li, D., Hua, S., & Sheng, V. S. (2023). A Survey on Image Semantic Segmentation Using Deep Learning Techniques. *Tech Science Press (Computers, Materials &Continua)*, *74*(1), 1941–1957. https://doi.org/10.32604/cmc.2023.032757

Filho, J., Nunes, L., & Xavier, J. (2022). iCorrVision-3D : An integrated python-based open-source Digital Image Correlation Software for in-plane and out-of-plane measurements. *Journal SoftwareX*, *19*(101132), 1–7. https://doi.org/10.1016/j.softx.2022.101132

Harikrishna, K., Nithin, A., & Davidson, M. J. (2025). Automated microstructural segmentation and grain size measurement of Al + SiC nanocomposites using advanced image processing techniques on backscattered electron images. *Materials Characterization*, *222*, 114845. https://doi.org/10.1016/j.matchar.2025.114845

Hong, J., Zhang, T., Zhou, R., Zhou, R., Ostikov, K. (Ken), Rezaeimotlagh, A., & Cullen, P. J. (2021). Plasma bubbles: a route to sustainable chemistry. *AAPPS Bulletin*, *31*(1), 1–14. https://doi.org/10.1007/s43673-021-00027-y

Hotaling, N. A., Bharti, K., Kriel, H., & Simon, C. G. (2015). DiameterJ: A Validated Open Source Nanofiber Diameter Measurement Tool. *Biomaterials*, *61*, 327–338. https://doi.org/10.1016/j.biomaterials.2015.05.015

Huang, B., Bates, M., & Zhuang, X. (2009). Super-resolution fluorescence microscopy. *Annual Review of Biochemistry*, *78*, 993–1016. https://doi.org/10.1146/annurev.biochem.77.061906.092014

Jardim, S., António, J., & Mora, C. (2023). Image thresholding approaches for medical image segmentation - short literature review. *Procedia Computer Science*, *219*, 1485–1492. https://doi.org/10.1016/j.procs.2023.01.439

John, A., Brookes, A., Carra, I., Jefferson, B., & Jarvis, P. (2022). Microbubbles and their application to ozonation in water treatment: A critical review exploring their benefit and future application. *Critical Reviews in Environmental Science and Technology*, *52*(9), 1561–1603. https://doi.org/10.1080/10643389.2020.1860406

Kim, Y., & Park, H. (2021). Deep learning - based automated and universal bubble detection and mask extraction in complex two - phase flows. *Scientific Reports*, *11*(1), 1–11. https://doi.org/10.1038/s41598-021-88334-0

Lewandowski, B., Ulbricht, M., & Krekel, G. (2018). An automated image analysing routine for estimation of equivalent diameter in high-speed image sequences with high accuracy and its validation. *Experimental Thermal and Fluid Science*, *98*, 158–169. https://doi.org/10.1016/j.expthermflusci.2018.05.016

Rayleigh. (1879). XXXI. Investigations in optics, with special reference to the spectroscope . *The London, Edinburgh, and Dublin Philosophical Magazine and Journal of Science*, *8*(49), 261–274. https://doi.org/10.1080/14786447908639684

Stelzer, E. H. K. (1998). Contrast, resolution, pixelation, dynamic range and signal-to-noise ratio: Fundamental limits to resolution in fluorescence light microscopy. *Journal of Microscopy*, *189*(1), 15–24. https://doi.org/10.1046/j.1365-2818.1998.00290.x

Xiong, X., Wang, B., Zhu, W., Tian, K., & Zhang, H. (2019). A review on ultrasonic catalytic microbubbles ozonation processes: Properties, hydroxyl radicals generation pathway and potential in application. *Catalysts*, *9*(1), 1–18. https://doi.org/10.3390/catal9010010